Moisture cycles of the forest floor organic layer (F and H layers) during drying

D. M. Keith,[1] E. A. Johnson,[1,2] and C. Valeo[2,3]

Received 16 March 2009; revised 30 January 2010; accepted 26 February 2010; published 22 July 2010.

[1] The forest floor in many ecosystems consists of a partially decomposed organic layer (duff), which together with the litter layer comprises the boundary between the atmosphere and the mineral soil. Processes controlling the duff water budget during *dry periods* (which occur during most of the summer) were investigated using field monitoring, field flow exclusion manipulations, and coupled, multiphasic water and heat budget modeling. The objective of this paper is to model the significant processes that govern the dynamics of the duff water budget during drying. During dry periods the moisture content of the duff's F layer cycles diurnally with minimal moisture movement between the duff and mineral soil. Field exclusion of dew, lateral flow, and mineral soil flow suggests that diurnal drying cycles during the dry period are driven by diurnal atmospheric energy fluxes leading to coupled heat and mass fluxes within the duff. The fine root system and lateral flow do not typically influence drying. TOUGH2 was used to develop a one-dimensional, multiphasic (both liquid and vapor) coupled water and heat budget model which confirmed that the vertical moisture fluxes lead to diurnal cycles. The model reproduced duff drying patterns with Nash-Sutcliffe efficiencies and R^2 values greater than 0.910 and 0.970, respectively. Wavelet analysis indicates that the model and observed diurnal cycles in the upper layer's moisture contents are correlated at the 24 h scale. A model flux analysis reveals that lateral fluxes smaller than approximately 360 $mm^3\ h^{-1}$ would have little influence on the pattern of drying in the duff layer. Fluxes larger than approximately 5% of the total evaporative flux would slow duff drying and lead to behavior not observed in the field.

Citation: Keith, D. M., E. A. Johnson, and C. Valeo (2010), Moisture cycles of the forest floor organic layer (F and H layers) during drying, *Water Resour. Res.*, *46*, W07529, doi:10.1029/2009WR007984.

1. Introduction

[2] The forest floor in many ecosystems consists of a partially decomposed organic layer (duff) up to 30 cm thick. The duff, along with the litter layer, is the boundary between the atmosphere and the mineral soil. Duff consists of two distinct layers, a top fermentation (F) layer and bottom humus (H) layer, but does not include the litter layer. The litter, F, and H layers are gradients of decomposition. The F layer is composed of slightly decomposed organic particles whose origins remain recognizable, while the particles in the lower H layer are more decomposed and their origins are no longer discernable [*Johnson*, 1992]. The physical and hydrological properties are very different from the underlying mineral soils [*Laurén et al.*, 2000; *Laurén and Mannerkoski*, 2001; *Miyanishi*, 2001; *Weiss et al.*, 1998]. The duff layer is found in forested ecosystems from the boreal forest through to tropical mountain forests [*Miyanishi*, 2001]. Despite its widespread distribution, there has been relatively little study of the hydrology of the duff layer; the vast majority of forest hydrological studies have dealt with mineral soils [*Buttle et al.*, 2000, 2005].

[3] The duff layer plays a pivotal role in the hydrology of the forest due to its location at the interface of the mineral soil and the atmosphere. It is directly impacted by latent heat fluxes and it impedes evaporative fluxes from the underlying mineral soil [*Tamai et al.*, 1998], slowing the potential rate of drying in the mineral soil. The duff has a low thermal conductivity and acts as an insulator between the atmosphere and mineral soil, leading to a reduction in the temperature, temperature fluctuations, and thermal gradient in the mineral soil [*Bonan and Shugart*, 1989; *Van Cleve et al.*, 1983]. The steep thermal gradient within the duff layer may lead to large vapor fluxes. In addition, the duff at the surface can be affected by dew; during dry periods dew can be an important moisture input [*Engstrom et al.*, 2005; *Jacobs et al.*, 2006] influencing the process of duff drying.

[4] Lateral runoff through organic soils should lead to spatial variability of moisture at the hillslope scale [*Carey and Woo*, 1999; *Kim et al.*, 2005]. The water retention capability of the duff layer is highly variable, with more decomposed duff able to retain more moisture at a given matric potential [*Laurén and Mannerkoski*, 2001]. This can lead to

[1]Department of Biological Sciences, University of Calgary, Calgary, Alberta, Canada.
[2]Biogeoscience Institute, University of Calgary, Calgary, Alberta, Canada.
[3]Department of Civil Engineering, Schulich School of Engineering, University of Calgary, Calgary, Alberta, Canada.

0043-1397/10/2009WR007984

the bottom H layer having significantly higher moisture content than both the top (F) layer and the underlying mineral soil. Additionally, the water retention capability facilitates moisture redistribution within the duff layer more easily than between the duff and the mineral soil; this may lead to a disconnection between the duff and the underlying mineral soil.

[5] A disconnection between the duff layer and the mineral soil has been implicitly assumed in the models that have been developed to simulate the drying process within the duff layer for smoldering combustion in forest fires [*Fosberg*, 1975; *Van Wagner*, 1979, 1982]. These duff moisture models ignore the influence of the underlying mineral soil, focusing solely on the duff layer (as a single homogeneous layer) and uses inputs of only temperature, humidity, and precipitation. *Van Wagner* [1979] developed an empirical model that split the drying of the duff into two stages, the constant rate and falling rate periods [*Perry et al.*, 1984]. The model used a simple exponential drying formula with only temperature, humidity, and precipitation as variables. *Fosberg* [1975] developed a more complete numerical duff drying model that coupled heat and vapor transport within the duff. This model indicated that the drying process is controlled by moisture content, energy input, and temperature within the duff [*Johnson*, 1992]. While it has not been widely applied, Fosberg's model remains the most detailed process-based model developed specifically for duff drying.

[6] Drying processes are very complex at the surface of any porous media exposed to the atmosphere [*Milly*, 1984], and neither the Van Wagner nor the Fosberg model includes all of the important processes. These models were designed to simulate average daily values; thus processes that control the water budget during drying at shorter temporal scales were not considered. The near surface drying process is strongly coupled to diurnal energy fluxes, and the moisture and temperature fluxes often have a distinct diurnal pattern [*Jackson et al.*, 1973, 1974]. In dry conditions, the dominant processes near the surface include evaporative, liquid, and vapor fluxes [*Jackson et al.*, 1974; *Yamanaka and Yonetani*, 1999]. The relative importance of these processes depends on the moisture content and thermal gradients. The diurnal drying cycles decrease in amplitude with depth and, as depth increases, the cycles increasingly lag the surface cycles [*Jackson et al.*, 1973]. Multiphase coupled heat and mass transfer models have been developed for mineral soils to deal with these processes [*dos Santos and Mendes*, 2005; *Grifoll et al.*, 2005; *Liu et al.*, 2005]. These models build on the theoretical work of *Philip and De Vries* [1957] and *Luikov* [1975], simulating the movement of moisture and heat near the surface for one-dimensional flow in drying mineral soils.

[7] At the tree canopy and hillslope scales, different processes lead to variability in the duff moisture content. At the tree canopy scale, interception leads to sites under the canopy being drier than sites in the open [*Miyanishi and Johnson*, 2002; *Raaflaub and Valeo*, 2008]. Duff moisture has also been found to vary with hillslope position [*Miyanishi and Johnson*, 2002; *Samran et al.*, 1995], with the duff moisture content higher at the bottoms of the hillslopes [*Bridge and Johnson*, 2000; *Vo*, 2001].

[8] Lateral flow through organic soils is one mechanism that can lead to redistribution of duff moisture [*Carey and Woo*, 2001; *McDonnell et al.*, 1991], though the importance of lateral flow is variable throughout the year [*Kim et al.*, 2005; *Sidle et al.*, 2001]. In mineral soils, lateral redistribution has been shown to be a transient effect, and topography plays a less important role as the length between significant precipitation events, i.e., *dry periods*, increases [*Grayson et al.*, 1997; *Western et al.*, 1998]. During these dry periods in mineral soil, there is little or no lateral redistribution, and the mineral soil drying becomes *locally controlled* with vertical fluxes dominating [*Grayson et al.*, 1997]. As *Jackson et al.* [1973, 1974, 1976] found, vertical fluxes dominate the mineral soil water budget when diurnal drying cycles are evident; thus, the diurnal pattern of drying may indicate a period of local control in many ecosystems. Previous research on boreal forest duff by *Vo* [2001] has found that duff moisture budgets are largely controlled by vertical fluxes (local control) during dry summer periods in the boreal forest.

[9] The objective of this paper is to model the significant processes that govern the dynamics of the duff water budget during drying. Empirical data collected over two years in a coniferous forest were analyzed to suggest what processes control the duff water budget. The results of this analysis provided the basis for two manipulation studies designed to isolate specific processes (dew input, lateral flux, vertical flux from the mineral soil, and canopy interception) and determine their influence on the duff water budget. The two years of monitoring data and the manipulation studies were used to help parameterize a multiphasic, coupled heat and mass transfer water budget model (TOUGH2) [*Pruess*, 2004]. This is the first step toward the development of a watershed scale model, based on the TOUGH2 framework, focused on the hydrological response of the duff layer.

2. Materials and Methods

2.1. Study Area

[10] The field data were collected in the Marmot Basin Research Watershed located in the Kananaskis Valley of Alberta, Canada (NAD83 11U 629800 5645900). The watershed covers approximately 9.6 km^2, with a minimum and maximum elevation of 1585 m and 2838 m, respectively. The climate in the region is characterized by long, cold winters and cool summers. The annual precipitation in the watershed ranges from 660 mm near the outlet to over 1100 mm at high elevations [*Stevenson*, 1967]. Historically, 70–75% of the precipitation falls as snow. The majority of the moisture input is due to snowmelt and precipitation during the spring and late summer, with May and June experiencing the most precipitation. Throughout the remainder of the summer the basin dries out, with the main input being rainfall associated with convective storms.

[11] The basin's outlet stream is fifth order (as in the stream classification proposed by *Strahler* [1957]) and flow out of the basin has been measured between May and October since 1964 at a V notched weir. Peak discharge from the basin occurs in June with a maximum instantaneous flow rate of 3.4 m^3/s (1995) and the mean daily average flow varies from a low of less than 0.1 m^3/s during the fall to a high of 0.65 m^3/s in June.

[12] The forest cover within the basin consists primarily of conifers. The upper subalpine forest consists of Engelmann spruce (*Picea engelmannii* Parry) and subalpine fir (*Abies*

lasiocarpa [Hook.] Nutt.) from approximately 1700–2200 m. The lower subalpine forest, below 1700 m, is dominated by lodgepole pine (*Pinus contorta* var. *latifolia* Dougl.) and Engelmann spruce. The duff layer is found throughout the forested parts of the watershed; the thickness of the layer varying from 4 cm in lodgepole pine stands to 30 cm under the canopy in both the spruce and fir stands. The mineral soil in the forested part of the basin consists largely of well-drained Podzolic soils [*Soil Classification Working Group,* 1998]. The basin is covered in well-drained stony glacial tills to a depth of approximately 10 m, with an infiltration rate much greater than peak storm intensity [*Stevenson*, 1967]. The bedrock consists of sandstone, shale, and conglomerate beds.

[13] In the upper part of the watershed, groundwater flow parallels the steep topography at shallow depths, leading to occasional springs. Mid watershed, the flow of water is generally downward through the surficial deposits. Near the outlet of the basin, this flow is deflected back toward the surface and discharged [*Stevenson*, 1967].

2.2. Field Measurements

[14] Field data used for model calibration were collected from late-May until early September in 2006 and 2007 in a *P. engelmannii* stand at an elevation of 1852 m. The soil moisture was measured at five depths: F layer (2 cm below surface), H layer (2 cm above bottom of duff), mineral soil −5 (5 cm below bottom of duff), mineral soil −15 (15 cm below bottom of duff), and mineral soil −25 (25 cm below bottom of duff) using a Theta Probe (Delta-T-Devices, Cambridge, UK) which was calibrated for the duff according to manufacturer recommendations [*Keith*, 2008], a calibrated field installed theta probe has an overall accuracy of ± 0.05 m^3m^{-3}. The probes were installed horizontally in an undisturbed soil column, the hole dug adjacent to the probe installation was then backfilled with the original mineral soil and duff. The soil moisture was measured at 10 min intervals, and each probe measures a 75 cm^3 volume. Soil temperature was measured at four depths as above, excluding mineral soil at 15 cm and at 15 min intervals (ONSET 4 Channel data logger and temperature sensors, Bourne, Massachusetts).

[15] Net radiation (Kipp and Zonen NR-Lite Net Radiometer, Delft, The Netherlands), wind speed (Windsonic anemometer, Gill Instruments, Hampshire, UK), temperature, and humidity (HMP45C, Campbell Scientific, Logan, Utah) were measured 1.5 m above the ground. Data were recorded once per minute and stored as 15 min averages (Campbell Scientific CR10X data logger, Logan, Utah). Precipitation was measured within the stand in a canopy gap, and in a clearing located near the plot (Onset Corporation tipping bucket rain gauge) with the latter measurement used to represent the actual amount of precipitation. A standard meteorological station was also located near the base of the watershed at 1450 m. These data were used to calculate the evaporation rate at the surface of the F layer, see section 2.4.

[16] Two manipulations were performed to study the affect of dew, vertical fluxes, lateral fluxes, and the fine root system, on the diurnal pattern of duff drying. The manipulation to observe the influence of dew was carried out during a drying period in early September 2007. The dew manipulation plot was covered by a plastic tarp at a height of 30 cm and covered a surface area of approximately 1 m^2. All moisture that condensed on the tarp was routed downslope of the plots. The dew manipulation excluded dew from the surface of the duff using a clear plastic tarp above the surface to minimize the manipulation's influence on the heat budget. The moisture content of the duff was measured with soil moisture probes located in the F layer (2 cm below the surface) and the H layer (2 cm above the bottom of duff). The soil moisture was measured at 10 min intervals throughout the manipulation (Theta Probe Delta-T-Devices).

[17] The manipulations implemented to exclude the fine root system, vertical and lateral water movement, were put in place from mid-May to mid-September, 2007. The exclusion manipulation plot was 0.072 m^3 (0.3 m wide × 0.3 m deep × 0.8 m long) and was set up in a *P. engelmannii* stand. In this manipulation, the top 30 cm of forest floor were completely isolated from both lateral and bottom vertical fluxes by four metal plates surrounding the sample and one plate running underneath at a depth of 30 cm. A control plot located nearby measured the moisture content in the same stand. In both plots the moisture content was measured in the F layer (2 cm below the surface), H layer (2 cm above bottom of duff), and the mineral soil layer 5 cm below the bottom of the enclosure. The enclosure disconnected the duff from the surrounding soil and vegetation, and thus, effectively disconnected the fine root system from the surrounding vegetation.

2.3. Duff Drying Model

[18] During dry periods, duff drying processes are driven by the coupling of heat and mass transfer within the duff, and vertical fluxes (as opposed to both vertical and lateral fluxes) will dominate the duff water budget [*Grayson et al.*, 1997]. This is shown conceptually in Figure 1 and detailed equations are given in Text S1.[1] From Figure 1, the model is one-dimensional with the thickness of the F and H duff layers specified. Fluxes of water, both as vapor and liquid, are modeled using a multiphase version of Darcy's Law [*Pruess*, 1999]. Redistribution is driven by pressure gradients (matric potential) within the duff. The energy budget includes both conduction and convection. The duff layer is an excellent insulator (Table 1) and does not readily conduct heat, leading to a large thermal gradient across the duff layer. Convection is tied to the water fluxes within the duff. As the duff dries, water moves upwards from the cooler parts of the duff, leading to a small reduction in the temperature of the duff near the surface.

[19] TOUGH2 includes a coupled energy (heat) and mass (water) balance and was used to model the drying of the duff layer [*Pruess*, 1999, 2004]. In the model the duff layer is divided into F and H layers, the properties of which are given in Table 1. The rate of water accumulation in the duff layer is equal to the water flux across the surface of the layer. A source or sink term is used at the boundary layers to add or remove water from the boundary (i.e., evaporative flux at the atmospheric boundary at the top of the F layer). The coupling of vapor and liquid fluxes with the boundary conditions at the duff surface drives the drying of the duff.

[1] Auxiliary materials are available in the HTML. doi:10.1029/2009WR007984.

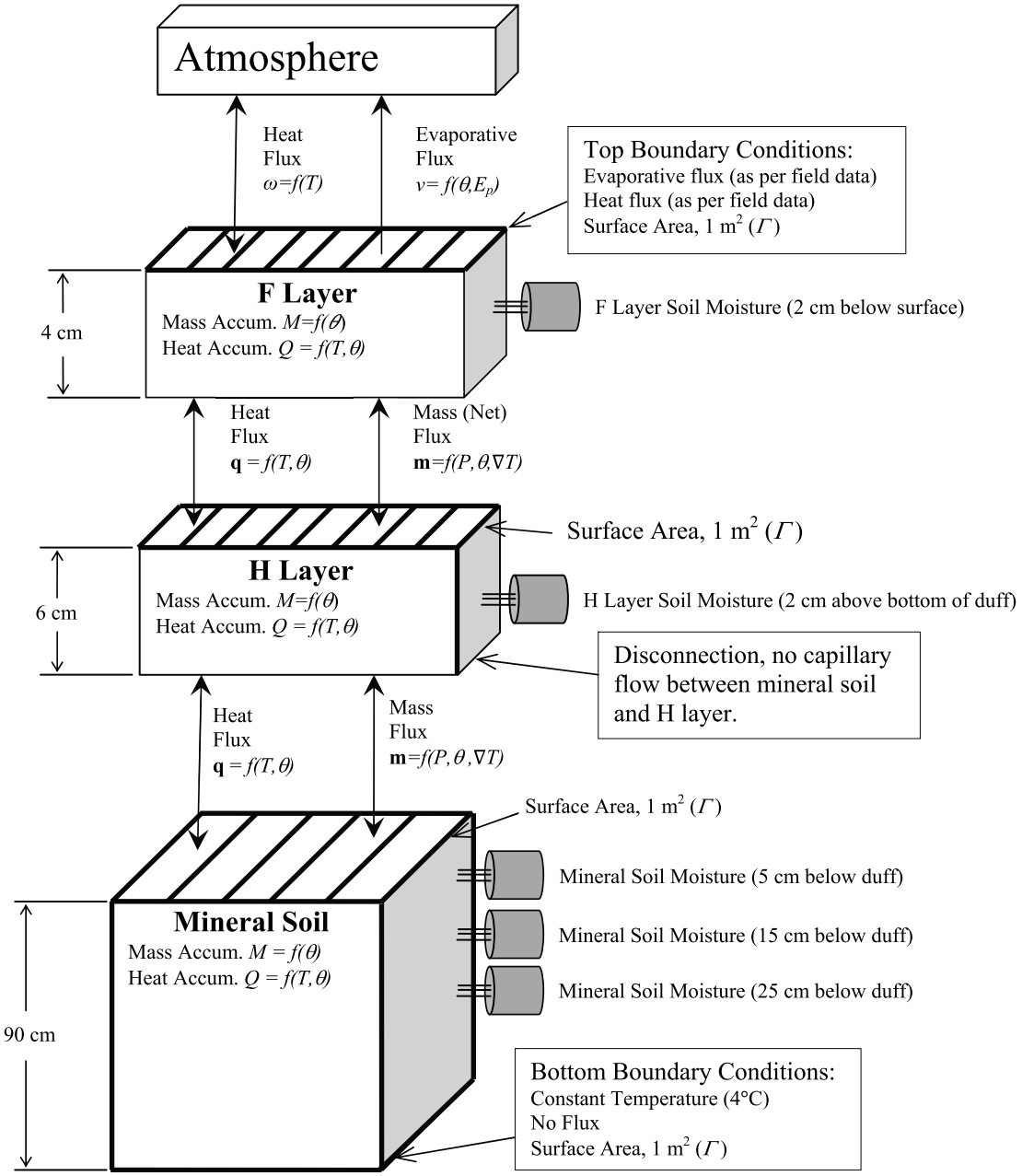

Figure 1. Conceptual representation of duff drying model.

[20] The vapor and liquid accumulated within a layer are dependent on the porosity of the duff layer. Higher porosity enables more vapor and liquid to accumulate in the duff. The flux within the duff is calculated using a multiphase version of Darcy's Law.

[21] Unsaturated flow within the duff via this mechanism is driven by gravity and pressure gradients (matric potential). Under a given pressure gradient the ability of fluid to flow through the duff varies. Higher duff permeability leads to increased flow through the duff under a given pressure gradient. The total water flux, due to Darcy flow, through the duff is the sum of the liquid and vapor fluxes. Highly porous materials such as duff lead to increased potential for diffusion, with the vapor phase diffusion coefficients being generally much larger than the liquid phase coefficients. While enhanced vapor diffusion in soils is a well known effect, it was not considered in this study.

[22] The dependence of tortuosity on saturation is calculated using the *Millington and Quirk* [1961] model. In this model, the tortuosity depends on the degree of saturation and the porosity of the duff layer.

[23] Analogous to the water balance, the rate of energy accumulated within the duff layer is the energy flux across the surface of the duff layer. A source or sink term can be used at the boundary layers to add or remove energy at the boundary (e.g., sensible heat flux at the top of the F layer). The energy accumulated by the duff matrix will vary with temperature, while the energy in the pore spaces depends on the quantity and temperature of vapor and liquid within the

Table 1. Model Parameters

Parameter	Value[a]	Units
F layer bulk density	110 (1)	kg m^{-3}
H layer bulk density	150 (1)	kg m^{-3}
F layer porosity	0.90 (1)	-
H layer porosity	0.86 (1)	-
F layer thickness	4 (1)	cm
H layer thickness	6 (1)	cm
Specific heat	1470 (2)	J kg^{-1}
F layer hydraulic conductivity	19.4 (3a)	cm s^{-1} ($\times 10^{-3}$)
H Layer hydraulic conductivity	10.4 (3b)	cm s^{-1} ($\times 10^{-3}$)
Thermal conductivity	0.45 (3c)	W m^{-1} K^{-1}
Moisture content when $E_e = 0$ (θ_0)	0.057 (4)	m^3 m^{-3}
Moisture content when $E_e = E_p$ (θ_{max})	0.6 (5)	m^3 m^{-3}

[a]Numbers in brackets indicate data source: 1: Field calculated data, obtained from samples used for soil moisture probe calibrations. 2: Specific heat of an organic soil [*Perry et al.*, 1984]. 3: Selected due to the similarity in thickness of organic layer, composition of the layers, the bulk density between the study sites. 3a: Saturated hydraulic conductivity, for the top 5 cm of the organic soil [*Hinzman et al.*, 1991]. 3b: Saturated hydraulic conductivity between 5 and 10 cm depth [*Hinzman et al.*, 1991]. 3c: Thermal conductivity at field capacity [*Hinzman et al.*, 1991]. 4: (θ_0) Minimum water content of the duff layer, based upon field data for the minimum observed moisture content in the F layer. 5: (θ_{max}) Moisture content when actual evaporation rate is equal to potential evaporation rate, parameter fitted to calibrate the model.

pores. These processes are modeled using the specific internal energy of the fluid which is a function of the physical properties, the phase, and the temperature of the fluid. The energy flux within the duff is modeled with both convective and conductive components.

[24] Conduction within the duff is dependent on the thermal properties of the duff layer and the duff temperature gradient. Duff has a low thermal conductivity, and is an excellent insulator when dry. As the water content in the duff layer increases the thermal conductivity will also increase, reducing its insular properties. Convection through the duff is due to the energy flux resulting from the movement of vapor and liquid; as the mass fluxes increase so will the energy fluxes within the duff layer.

2.4. Model Parameterization and Initial and Boundary Conditions

[25] The parameters used in the simulations are given in Table 1 and relevant equations are provided in Text S1. The parameters are based on field observations or previously measured values from the literature. The initial conditions for each simulation period were based upon the moisture content and temperature data measured in the field. At the bottom boundary, a constant temperature of 4°C and a no flux condition were assumed. This assumption in this initial modeling attempt provides for a useful simplification, particularly given there was insufficient information available on the hydraulic properties of the soil layer. At the atmospheric boundary the heat flux was based upon a simple heat balance using atmospheric temperatures. To calculate the mass flux from the F layer the Penman equation was used to model the potential evaporation rates [*Penman*, 1948]. Driven by net radiation flux and air drying power, the air drying power incorporates both the air drying power and vapor pressure deficit as part of the Penman model. The Penman equation assumes that a sufficient amount of water can be supplied to the duff surface. In the field this is rarely the case for the duff, and the actual evaporation rate is below the potential rate calculated using the Penman equation. A simple model was used to account for the influence of the duff moisture deficit [*Brutsaert*, 2005]:

$$\delta = \frac{\theta - \theta_0}{\theta_{max} - \theta_0} \quad (1)$$

where δ is the fraction of potential evaporation realized as actual evaporation, θ is the duff moisture content (m^3 m^{-3}), θ_0 is the duff moisture content when actual evaporation rate = 0 (m^3 m^{-3}) and θ_{max} (m^3 m^{-3}) is the duff moisture content when actual evaporation rate (E_e in mm h^{-1}) equals the potential evaporation rate (E_p in mm h^{-1}). Combining equation (1) with the Penman Equation in Text S1 yields the actual evaporation rate as

$$E_e = 3.6 \times 10^6 \frac{\delta E_p}{\rho L} \quad (2)$$

where ρ is the water density (kg m^{-3}) and L is the latent heat of vaporization (J kg^{-1}).

[26] The numerical methods described here are found in the TOUGH2 package [*Pruess*, 1999, 2004]. The governing equations and boundary conditions are solved numerically [*Narasimhan and Witherspoon*, 1976]. The continuous form of the conservation equations are made discrete using the integral equations. No conversion into partial differential equations occurs, and the method used is an integral finite difference.

2.5. Analysis of Model and Manipulations

[27] The simulated moisture content of both the F and H layers was compared to the actual moisture content using two measures. Nash-Sutcliffe efficiency was used to compare the actual and modeled moisture content in both the F and H layers [*Nash and Sutcliffe*, 1970]; this measure depends upon both the shape of the time series and the actual values of the data. Nash-Sutcliffe efficiency values range from $-\infty$ to 1, where 1 represents a perfect fit of model to observations. The coefficient of determination R^2 was used as an additional measure of the timing of the fit between the model and observations.

[28] The F layer time series were non stationary, i.e., they had periodic signals that changed in both frequency and amplitude over time, therefore they could not be compared with traditional time series methods, and thus, wavelets analysis was employed [*Torrence and Compo*, 1998]. Wavelet analysis decomposes a time series into both time and frequency space; thus it represents the frequency of the signal while retaining information about the time parameter. Wavelet analysis results in edge effects that are delineated using a cone of influence (COI): within this cone the influence of edge effects are minimal, while outside the cone edge effects become significant and the results are typically ignored.

[29] A cross wavelet transform was used to compare the results from the field data for the F layer to: a) the results from the dew manipulation, b) the enclosure manipulation and c) modeled results for the F layer. The wavelet analysis was used to determine if the diurnal cyclic signal between the two time series was significantly correlated, at what time period they were correlated (i.e., 24 h), and to determine if

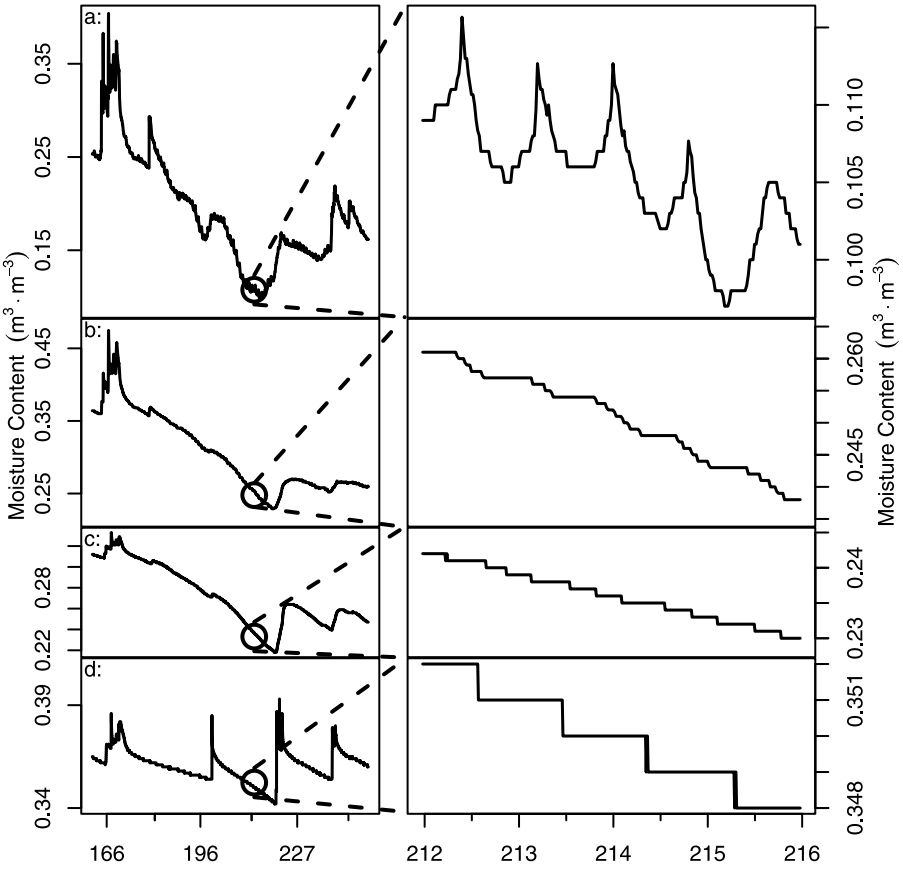

Figure 2. Moisture content at various depths for the period of 2007 Julian day 166 (June 15) to roughly 241 (September 15th). The circled region (July 31st to August 4th or days 212–216) is shown in detail on the right. (a) Moisture content of the F layer. (b) Moisture content of the H layer. (c) Moisture content at a depth of 5 cm. (d) Moisture content at a depth of 25 cm.

there was a time lag between the signals (i.e., does the moisture content peak at the same time, or is there a delay).

[30] These results were subsequently used with a wavelet coherence transform. This analysis examines the coherence of a cross wavelet transform yielding the correlation coefficient between the two time series in time-frequency space. Both of these wavelet transforms used a Morlet wavelet for analysis [*Maraun and Kurths*, 2004]. The analysis also includes a measure of synchrony between the time series; these phase data were used to determine whether there was a delay between the cycles in these time series. The data were found to be normal in the wet and dry periods and thus, significance testing of the coherence between time series was based upon the Monte Carlo method of *Maraun and Kurths* [2004] at a 95% confidence level.

3. Results

3.1. Field Monitoring

[31] Figure 2a shows the temporal variability in duff moisture from late May to early September 2007 (the results of the 2006 and 2008 field seasons were similar) for the F layer. Two patterns are evident: first, there are short periods when duff water content increases rapidly because of precipitation which are followed by rapid drying due to breaks in rainfall or a reduction in rainfall intensity. Second, and the focus of this paper, are the extended periods with diurnal cycles in the F layer of the duff that exist in most of the period from July through to September as in Figure 2a. These diurnal cycles dampen with depth, and there is no evidence of a diurnal drying pattern in the mineral soil shown in Figures 2c and 2d. The circled region in Figure 2a shows a detailed example of the diurnal moisture cycles and how these cycles follow a predictable pattern in the F layer. During the mid-morning the moisture content increases typically from 07:00–10:00 (all times MDT); with a peak moisture content occurring in the early afternoon at approximately 12:30–13:00 (see Figures 2a and S1 depicting the 24 h period from 6:00 A.M. on July 31st to 6:00 A.M. on August 1st). The majority of the decrease in the F layer moisture content occurs during the afternoon and evening at approximately 13:00–20:00. In the F layer, the moisture content increases up to 5% of the total moisture content during the morning. The increase in the F layer moisture content can be a significant fraction of the total decrease in moisture content during the afternoon as shown in Figure 2a. The net effect of these cycles is to slow drying in the F layer.

[32] Figure 2b shows that in the H layer there is no cycling. The moisture content does not increase during any precipitation free 24 h period, but the H layer begins to dry approximately at the same time that the F layer begins to increase in moisture content, strongly suggesting that the H layer is the source of the moisture moving into the F layer.

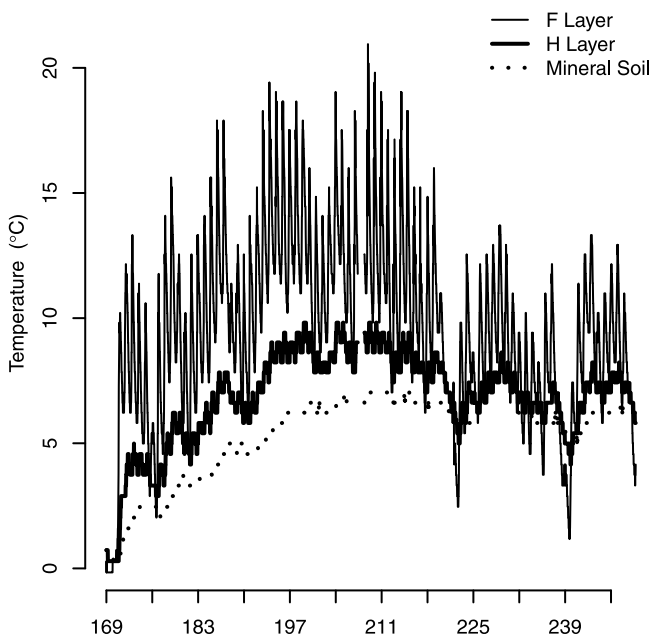

Figure 3. Measured diurnal temperature cycles in the F layer, H layer and mineral soil at a depth of 5 cm during the 2007 field season for days 169–246 (June 18th to September 3rd).

Also, Figures 2a and 2b show that the moisture content of the H layer is generally higher than that of the F layer. Additionally, the mineral soil shows no sign whatsoever of a diurnal pattern of drying (Figures 2c and 2d) at any point during the season.

[33] Field data from 2007 shown in Figure 3 reveal the substantial temperature gradient across the duff layer, with the F layer up to 10 degrees warmer than the H layer during the afternoon. Large diurnal temperature cycles of as much as 10°C in the F layer were observed throughout the season while the H layer was much less variable, cycling diurnally by approximately 1°C. Figure 4a demonstrates that the temperature gradient between the F and H layer peaks in the early afternoon (1–2 P.M. though this is somewhat seasonally dependent) on most days. This peak comes after the peak in the F layer moisture content and the evaporative flux calculated from meteorological data, both peaking by 1 P.M. as shown in Figures 4b and 4c. The evaporative flux is increasing as the moisture content of the F layer increases. The F layer moisture content appears to increase with increasing evaporative flux. This suggests that evaporation is driving moisture redistribution within the duff, and as suggested in Figure 2, the source of this moisture seems to be the H layer

3.2. Manipulation Results

[34] The exclusion manipulations were performed to look at the influence of dew, vertical fluxes, lateral fluxes, and the fine root system on the diurnal pattern of duff drying in

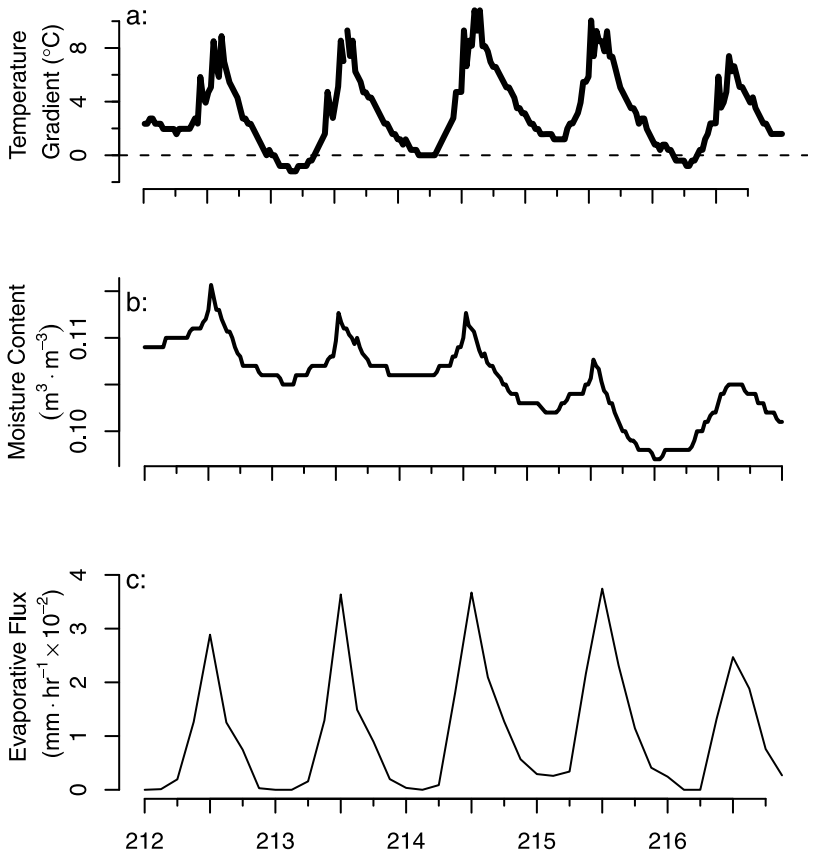

Figure 4. Detailed view of (a) the F-H temperature gradient, (b) the F layer moisture content, and (c) the Penman calculated evaporative flux, from July 31st to August 4th 2007 (days 212–216).

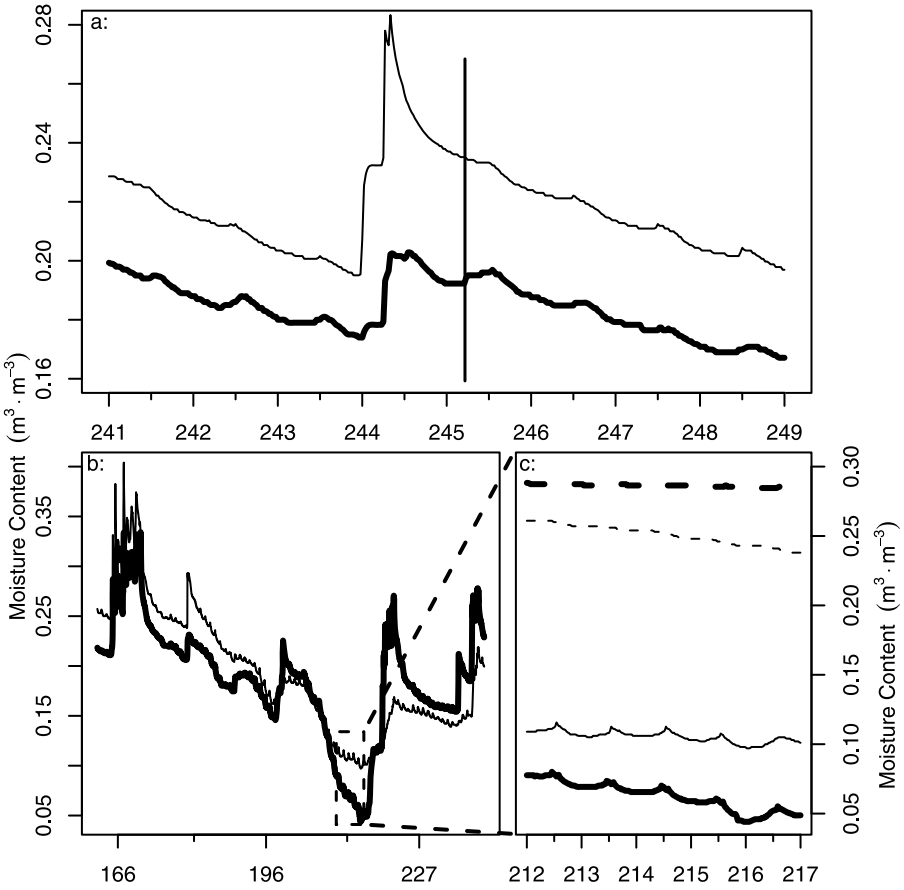

Figure 5. (a) Moisture content of the F layer for the control and exclusion manipulation from roughly June 15th (day 166) to September 15th (day 241). The vertical line represents beginning of the exclusion manipulation experiment. (b) Moisture content of the F layer of enclosure manipulation for the control and enclosed locations during the 2007 field season, boxed region between July 31st and August 4th shown in Figure 5c. (c) Moisture content of the F and H layers for the control and enclosure. The thin line represents the control plot and the thick line is the manipulation data, while the solid and dashed lines represent the F and H layers respectively.

the F layer. The initial increase in the F layer moisture content (Figures 2a and S1) occurs near the time that dew forms (during the dew manipulation dew was observed throughout the experimental area by 6:00 A.M. each day and shown in Figure S1), and consequently dew could be the process leading to the increase in duff moisture content during the morning. Few studies of dew have been done in mid latitudes, though there is some evidence it is an important seasonal input in dry ecosystems [*Engstrom et al.*, 2005; *Jacobs et al.*, 2006]. The results of the dew manipulation in Figure 5a show that diurnal cycling continues despite the exclusion of dew. The experiment begins following a rainfall event on September 1st, i.e., to the right of the vertical line. Qualitatively the response of the control and the dew exclusion manipulation show that there is no noticeable difference in response between plots. Wavelet analysis (Figure S2) was performed to quantitatively compare the behavior of the plots before and during the manipulation. The wavelet analysis indicates that there is a significant correlation between the cycles in both the control and manipulated plots and that this correlation did not change significantly from data collected before the barrier was put in place (to the left and right of the vertical line. There appeared to be little effect on the diurnal cycles when dew was excluded from the duff layer; thus implying that dew may not be contributing to the duff water budget during drying. Note that the wavelet analysis, see Figures S2 and S3, clearly picks up the signal of the rainfall event, with the response of both plots becoming highly correlated at almost all time scales during the rainfall event on September 1st.

[35] The completely enclosed manipulation blocked vertical fluxes from below the enclosure, lateral fluxes, and isolates the fine root system from the surround vegetation thus blocking the majority of transpiration and hydraulic lift. Moisture uptake from the duff layer to the fine root system could be driven by transpiration during the day. During the evening when transpiration ceases, movement of moisture from vegetation into the duff layer via the roots, known as hydraulic lift, could lead to diurnal recharge of duff moisture [*Caldwell et al.*, 1998]. Hydraulic lift moves water from areas of higher water potential, the vegetation roots, into areas of low water potential, the duff layer, increasing the moisture content near the surface [*Caldwell et al.*, 1998]. Transpiration would lead to a reduction in duff moisture content near sunrise, peaking in the afternoon and near sunset, while hydraulic lift would lead to increases in

the soil moisture content overnight when evaporation rates are lowest. The combination of these two processes could lead to diurnal cycles in duff moisture content (Figure S1).

[36] Despite the removal of the vertical and lateral fluxes and fine roots, the timing and pattern of the diurnal cycling between the completely enclosed and control plots were similar throughout the dry periods (Figure 5b), indicating that fluxes from outside the volume of the enclosure did not contribute to the diurnal drying of the duff. Wavelet analysis again showed a significant correlation between the cycles for each location at the 24 h period throughout the dry periods during the summer of 2007 (Figure S3). Throughout the majority of the season the enclosure did not significantly influence the processes controlling the water budget of the duff layer during dry periods. This suggests that the moisture entering the F layer as observed by the diurnal fluctuations during drying periods was coming from within the enclosure. This indicates that the diurnal cycling was driven by fluxes of moisture from the moist bottom H layer to the F layer, and that there was typically a disconnection between the H layer and the underlying mineral soil during dry periods with little moisture moving from the mineral soil into the duff.

[37] Wavelet analysis confirms the diurnal cycles between the control and enclosed plots are highly correlated at the 24 h scale during the dry periods (see Figure S3) with little difference in phase (timing) of the cycles between the plots. As discussed above, multiple rainfall events show a clear signal as the correlation becomes significant at most time scales. Additionally, Figure S3 shows that there is no correlation in the plots during the transition period between the end of the rainfall and the beginning of the diurnal cycles. This wavelet analysis is able to resolve the dry periods when diurnal cycles occur within both plots.

[38] During one short period (July 29th to August 4th) there was a difference in the drying pattern between the enclosure and the control for the F layer as shown in Figure 5b and magnified in Figure 5c. The diurnal pattern between the two plots for the F-layer is similar and only the rate of drying of this six day period is slightly different. Figure 5c also shows that in this same time period, the enclosure plot's H layer, is losing very little moisture in comparison to the control plot. This implies a lack of movement of moisture from the H layer to the F layer in the enclosure (in comparison to the control plot) during this period. As can be seen in Figure 5b, the enclosure's moisture content drops to its lowest level during this period and is close to the error of the soil moisture probe. At very low levels of moisture content, thermal gradients are insignificant drivers of vertical moisture fluxes; thus, the temperature gradient between the F and H layer contributed less to driving flux from the H layer to the F layer. While the supply of moisture to the F layer was reduced from the bottom of the H layer (where the moisture content remained relatively stable), moisture from regions between the probes apparently still contributed moisture to the F layer as the diurnal cycles continued, albeit in a reduced state.

3.3. Model Results

[39] Simulations were performed to determine whether the fluxes identified by the manipulations could replicate the field measurements of duff moisture content in both the F and H layers. The simulations were based upon field data collected during the two longest dry periods in the summer of 2007 (Period 1: July 3rd–July 16th, Period 2: July 21st–August 4th). As suggested by the field observations and the manipulations the duff layer was modeled with no liquid movement between the mineral soil and the H layer in these simulations and the model parameters are given in Table 1. The parameters resulted from a calibration by hand (to achieve the highest Nash and Sutcliffe efficiency possible between observed and modeled values) on the period of June 25th to July 8th, 2006 and achieved a Nash and Sutcliffe efficiency of 0.93. Vapor fluxes were modeled between the mineral soil and H layer, but they were less than 1% of the net vapor flux between the F and H layer. The results were compared to the actual moisture content from these two periods. These simulations also quantified the liquid and vapor fluxes and their influence on the diurnal cycles in F layer moisture content.

[40] The simulation results for the two dry periods closely recreated the pattern of drying in the duff for both the F and the H layers (Figure 6). The F layer Nash-Sutcliffe efficiencies were 0.920 and 0.961 for Periods 1 and 2 respectively, while the R^2 values were 0.970 and 0.982. For the H layer Nash-Sutcliffe efficiencies of 0.979 and 0.910 were obtained for Periods 1 and 2 respectively, while the R^2 values was 0.980 for both periods. Wavelet analysis shown in Figures S4 and S5, indicates that the actual and modeled diurnal cycles are highly correlated during both periods at the 24 h scale. This analysis also shows that there is a slight phase differences between the plots, with the model F layer moisture content peaking after the actual peak. This slight bias is likely due to the simplified Penman based evaporative boundary model.

[41] The drying pattern's local control [cf. *Grayson et al.*, 1997] can be simulated by coupling the liquid and vapor fluxes from the H and F layers driven by diurnal evaporative fluxes. Positive fluxes indicate movement from the H to the F layer, while negative fluxes indicate movement from the F to the H layer. The liquid fluxes redistributed moisture from the H layer to the F layer as seen in Figure 7a, while the smaller vapor fluxes followed the thermal gradient, redistributing moisture downward. The liquid and vapor fluxes had very strong diurnal cycles, with peaks in both cycles occurring during the afternoon. The diurnal moisture cycles in the F layer were due to the net flux within the duff coupled with evaporative fluxes. The F layer moisture content increased throughout the morning when the evaporative flux was smaller than the net flux from the H layer to the F layer as shown in Figure 7b. During the afternoon and evening the F layer dried because the evaporative fluxes were larger than the net flux in the duff. This occurred despite the peak in the net flux during this time. It is this transport limitation that results in the drying of both the F and H layer during the afternoon and evening. These results indicate that diurnal cycling of meteorological fluxes lead to variable liquid and vapor fluxes within the duff and the coupling of these processes leads to diurnal cycling in the F layer.

[42] A model flux analysis was performed to determine the magnitude of external moisture fluxes that would affect the F layer budget. The fluxes were added to the H layer to simulate lateral (or vertical) fluxes into the duff layer from the surrounding soil column. The results of these simula-

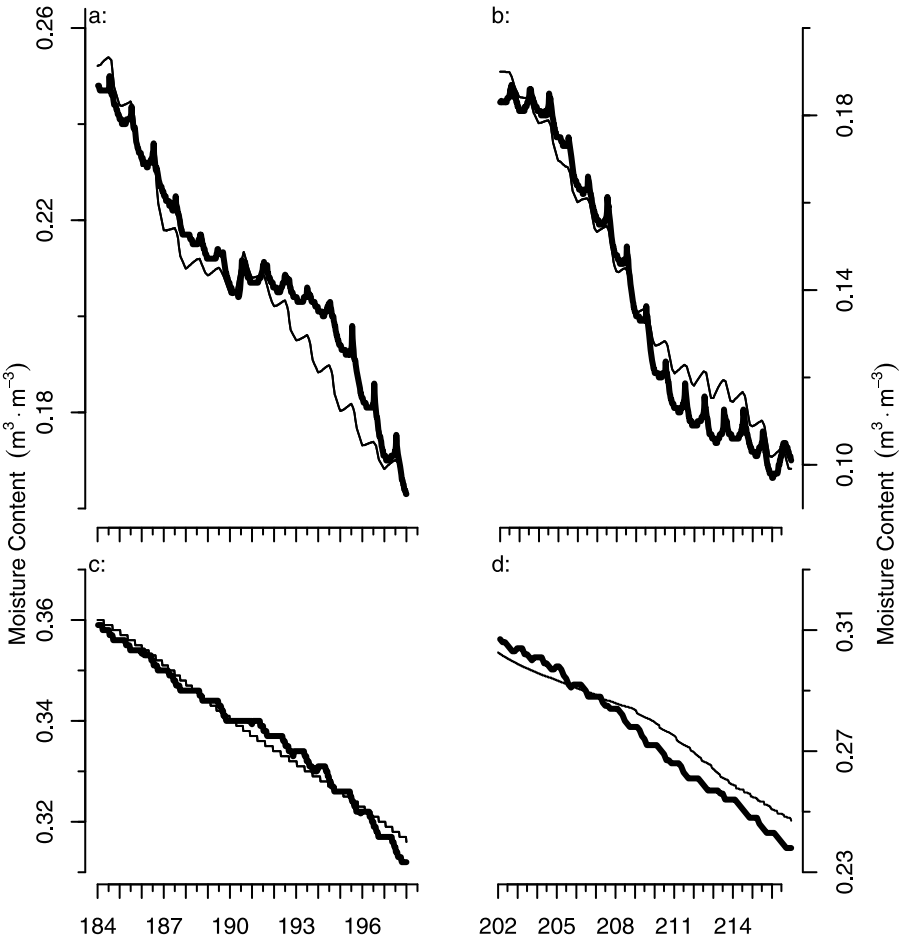

Figure 6. Modeled and actual moisture content for (a) F layer for the period 3–17 July 2007 (days 184–198), (b) F layer for the period 21 July to 4 August 2007 (days 202–216), (c) H layer for the period 3–17 July 2007, and (d) H layer for the period 21 July to 4 August 2007. The thin line represents the model while the thick line is the actual data.

tions indicate that small flows of moisture (<360 $mm^3\ h^{-1}$) have little influence on the duff water budget (Figure 8a). Moderate-sized fluxes (360–1440 $mm^3\ h^{-1}$) slow the overall drying rate in both the F and H layers and lead to a slight increase in the amplitude of the diurnal cycles. When the size of the moisture flow is greater than approximately 5–10% of the peak evaporative fluxes (in this simulation >1440 $mm^3\ h^{-1}$), the drying rate slows greatly, and little drying occurs throughout the duff (as in Figure 8a). In the H layer the additional flow has less overall influence than on the F layer, though the overall trend is similar to the F layer, with little drying occurring during larger fluxes (Figure 8b).

4. Discussion

[43] The one-dimensional coupled heat and mass transfer model simulation and the empirical evidence from the manipulations demonstrated that duff drying is largely driven by diurnal evaporative fluxes during dry periods. These fluxes lead to diurnal vapor and liquid fluxes within the duff layer. Throughout the morning, the net flux from the H layer to the F layer is larger than the evaporative flux; this leads to the increase in the F layer moisture content. During the afternoon, the evaporative flux becomes larger than the flux from the H to the F layer, leading to drying throughout the duff layer. This is the process that leads to the diurnal moisture cycles within the duff.

[44] Similar processes have been found to cause diurnal cycles in mineral soils [*Hillel*, 1975; *Jackson et al.*, 1973; *Yamanaka and Yonetani*, 1999], while in our study no diurnal cycling was observed in the mineral soil. These mineral soils all seemed to have little or no duff layer, and focused upon the short-term drying behavior of a range of relatively dry mineral soils. The diurnal cycles were generally quite similar in the duff and these mineral soils, though there were apparent differences in the amplitude and timing of the cycles. The amplitude of the cycles in the mineral soil was almost an order of magnitude larger at the top of the soil (up to 0.1 $m^3 m^{-3}$) [*Jackson et al.*, 1974] than was found in the duff layer. As depth increased the amplitude of the diurnal cycles decreased and there was a time lag found at depths as little as 1 cm in the mineral soil [*Jackson et al.*, 1974]. These lags delayed the timing of the cycles by approximately 1–2 h and reduced the amplitude of the cycles by approximately 50% at a depth of just 1 cm [*Jackson et al.*, 1974]. Our study measured the average moisture content in the top 4 cm of the duff layer, so that both the

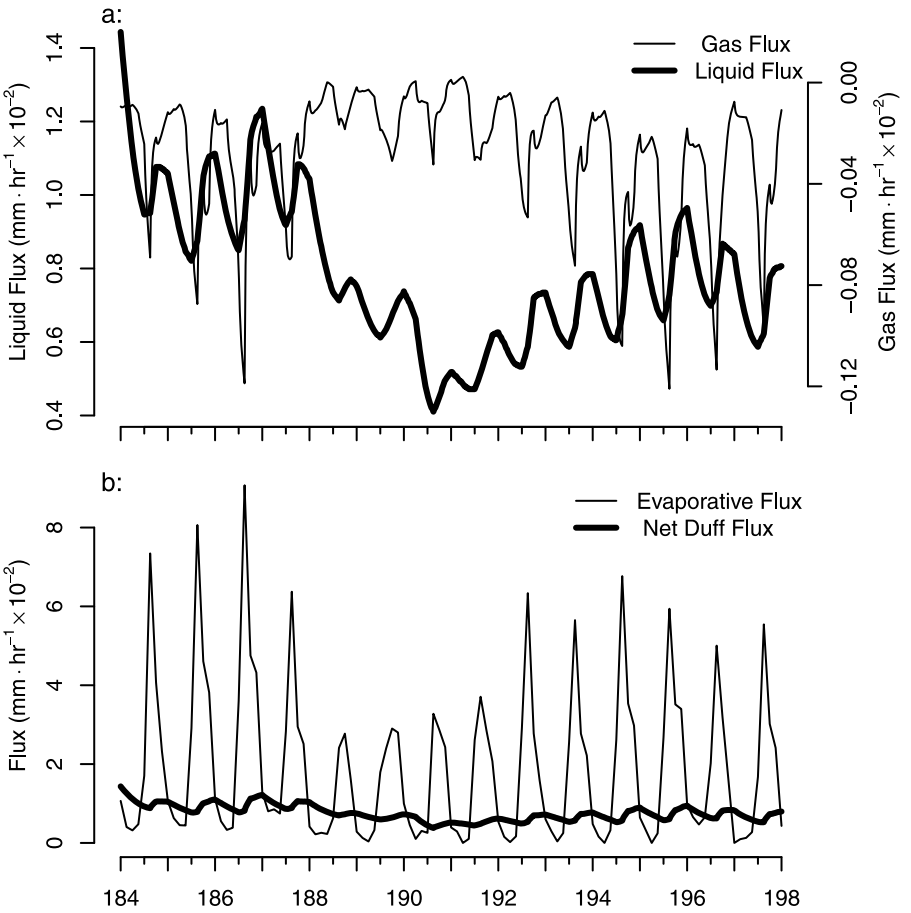

Figure 7. (a) Simulated gas and liquid fluxes between the F and H layer for 3–17 July, 2007. (b) Simulated net flux of moisture from the H layer to the F layer compared to the calculated evaporative fluxes.

time lag and the smaller amplitude cycles are consistent with their findings for mineral soil.

[45] In mineral soils the moisture fluxes near the surface dropped off rapidly as the soil dried, while fluxes in deeper layers (9 cm depth) did not change significantly [*Jackson et al.*, 1973]. The fluxes in the deeper layers resulted from the redistribution of moisture from as deep as 35 cm [*Jackson et al.*, 1973]. Overall the net fluxes in mineral soils were approximately an order of magnitude larger than those found in the duff layer [*Jackson et al.*, 1974]. In our study, there was a disconnection between the bottom H layer and the underlying mineral soil, resulting in minimal capillary fluxes between these layers during dry periods. Overall, there was less moisture available for redistribution within the duff because of this disconnection. The disconnection was likely the cause of the lower fluxes, and could also lead to smaller amplitude cycles in the duff layer due to a supply limitation. The net fluxes in both the duff (this study) and mineral soils [*Jackson et al.*, 1974] were due to a combination of liquid and vapor fluxes, with the vapor fluxes driven largely by vertical thermal gradients and the vertical liquid fluxes driven by redistribution due to evaporative drying.

[46] During these dry periods, the duff is *locally controlled* since vertical fluxes dominate the duff water budget [cf. *Grayson et al.*, 1997]. Local control has often been assumed to occur when potential evaporation exceeds precipitation [*Western et al.*, 1999], but near the surface the pattern of drying is a more precise indicator of local control. Shortly after large inputs of moisture (precipitation or snowmelt), liquid flow, both vertical and lateral, will dominate the budget, as the increased hydraulic conductivity of the duff enables rapid redistribution of moisture. Thus, there is the *potential* for lateral flow through the duff layer. Following this there is a short (approximately 12–24 h) transition phase as the duff dries in which the relative importance of the diurnal fluxes is increasing and the diurnal drying pattern is becoming evident. After a large precipitation event the F layer is under local control within 48 h; although in the H layer the transition can take an additional 24 h. During dry periods small precipitation events are not sufficient to remove local control in the duff layer; therefore, throughout most of the summer the duff water budget is dominated by vertical fluxes and is locally controlled.

[47] The model flux analysis indicates that vertical flow from the mineral soil and horizontal flow from the duff could lead to spatial variability in the duff moisture content. Small lateral flows less than 360 mm^3 h^{-1} into the H layer would not alter the budget significantly. Moderate flows, between 360 and 1440 mm^3 h^{-1}, through the duff could influence the budget and also lead to an increase in the amplitude of the diurnal cycles within the duff layer without altering the pattern of drying significantly. Flows greater than approximately 5–10% of the peak evaporative flux

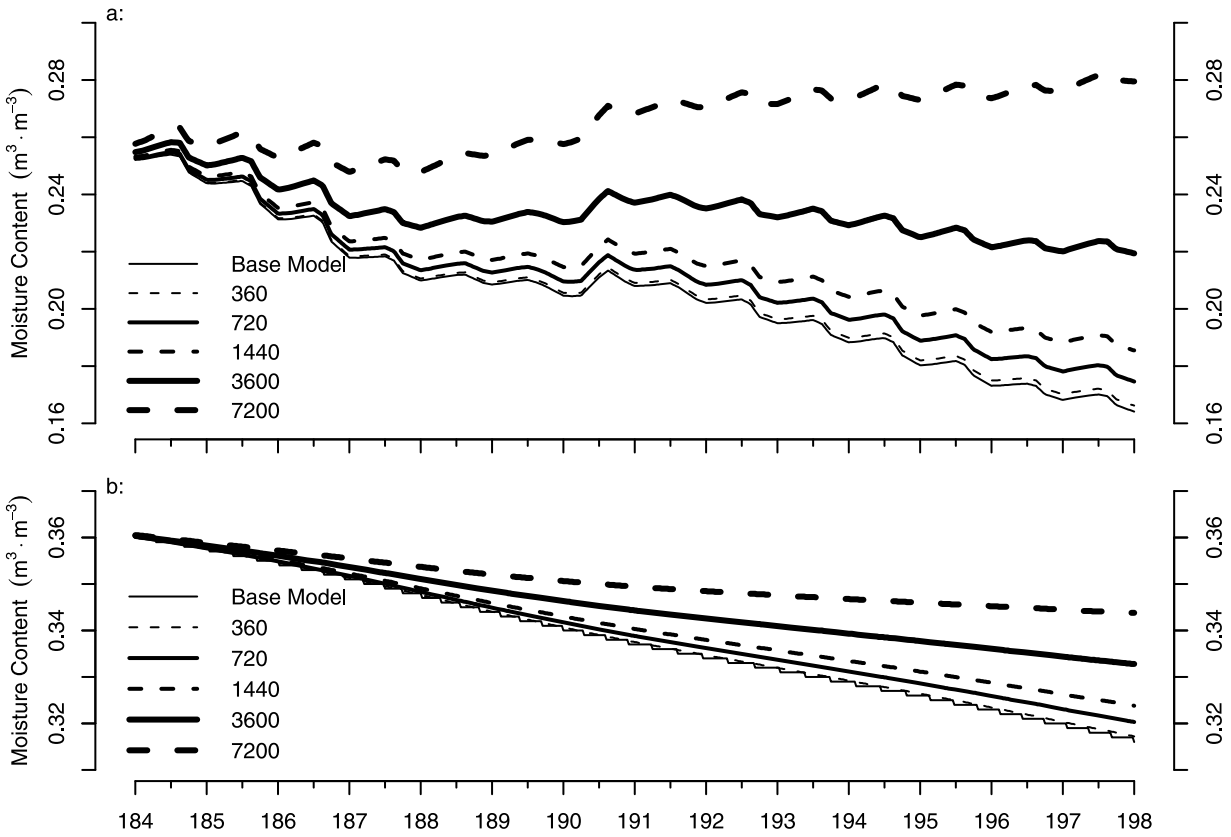

Figure 8. Results of model flux analysis (a) for the F layer and (b) for the H layer for 3–17 July, 2007. The flow rates in the legend are $mm^3\ h^{-1}$ and were added to the H layer. The base model includes no flow into the H layer from the surroundings (i.e., mineral soil or lateral flow through the duff).

could lead to major reductions in the drying that occurs in the duff layer. The size of these flows indicates that the spatial moisture redistribution would be on the order of centimeters to a meter during these dry periods. These flows have a larger impact on the budget at lower moisture contents as evaporative fluxes are smaller in drier duff (e.g., Figure 8, July 10–17).

[48] Throughout the majority of the season, these flows are either not occurring or are too small to have an observable influence on the water budget. This analysis reveals that moderate flows at very short scales could lead to spatial variability in duff moisture during dry periods. These flows were not directly observed in the field, though comparison of the model flux analysis with the enclosure manipulation suggests that moderate flows to the H layer could lead to spatial variability in the field. Further empirical studies are needed to determine the source, magnitude, and frequency of external fluxes into the H layer during dry periods.

[49] The results of the manipulations also reveal that transpiration and resulting water uptake by the fine root system did not impact duff drying during dry periods. This, in combination with the minimal amount of lateral flow and the disconnection of the underlying mineral soil, indicates that evaporative flux is a major driver of the duff water budget during the majority of the dry periods. Generally, separation of evaporative fluxes from non-biological sources (i.e., duff, soil, open water) and biological sources (i.e., transpiration from plants) is difficult and numerous methods have been proposed to estimate these fluxes [*Cooper et al.*, 1983; *Ritchie*, 1981]. Our results indicate that, in forested ecosystems with a thick duff layer (≥10 cm) and minimal understory vegetation, drying of the duff layer is largely driven by non-biological evaporative fluxes.

[50] The mismatch in the amplitude and timing of the Penman evaporation fluxes in Figure 6 is the reason for the slight bias in the model results for the F layer. The Penman model was used to estimate the evaporative fluxes because of its mechanistic basis and the widespread availability of necessary meteorological data. The Penman equation underestimates evaporative fluxes during the morning and overestimates the fluxes during the early afternoon. This causes a slight mismatch between the timing and amplitude of the diurnal cycles and can lead to over- or under-estimations of the moisture content. In dry conditions it has been found that the latent heat flux peaks earlier in the day than under wet conditions; further, the latent heat flux was found to peak before net radiation in dry soils [*Yamanaka and Yonetani*, 1999]. This diurnal variability of latent heat flux would lead to the observed discrepancy in the timing of the modeled diurnal cycles. Overall, the Penman method gives very good results using basic meteorological data. The great advantage of this method is that it can be used in locations where only basic meteorological data are available.

5. Conclusions

[51] The objective of this paper was to model the significant processes that govern the dynamics of the duff water

budget during drying. Field observations indicate that the process of drying within the duff layer is driven by diurnal evaporative fluxes that lead to diurnal moisture cycles in the duff layer. During dry periods the mineral soil has minimal influence on the drying processes within the duff; the duff and mineral soil effectively become disconnected. This disconnection is a temporal effect that occurs when there is little moisture input into the duff layer, but the timing of this disconnection *may* also be spatially variable.

[52] Model flux analysis indicates that relatively small fluxes of moisture into the H layer of the duff could lead to the spatial variability observed in the duff moisture content at scales of less than a meter. At larger scales, duff moisture content has been found to vary across hillslopes, with wetter locations found at the bottom of hillslopes. A potential mechanism leading to the hillslope variability is lateral flow through the duff during and shortly after a significant snowmelt or rainfall [*Carey and Woo*, 2001; *Kim et al.*, 2005]. To better understand the pattern of local control of the duff water budget, a spatially variable three-dimensional model is required.

[53] **Acknowledgments.** The authors would like to thank the reviewers for their insightful comments. This research was supported by a Natural Sciences and Engineering Research Council (NSERC) Discovery Grant and NSERC's GEOIDE Network of Centre of Excellence. The authors would also like to thank Lindsey Park, Heather Conquergood, Marianne Chase, Paul Moquin, Ellen Lea, Karen Yee, Laura Hickman, and Kelly Boyle for their assistance in the field and in the lab.

References

Bonan, G. B., and H. H. Shugart (1989), Environmental factors and ecological processes in boreal forests, *Annu. Rev. Ecol. Syst.*, *20*, 1–28, doi:10.1146/annurev.es.20.110189.000245.

Bridge, S. R. J., and E. A. Johnson (2000), Geomorphic principles of terrain organization and vegetation gradients, *J. Veg. Sci.*, *11*(1), 57–70, doi:10.2307/3236776.

Brutsaert, W. (2005), *Hydrology: An Introduction*, 1st ed., 605 pp., Cambridge Univ. Press, New York.

Buttle, J. M., I. F. Creed, and J. W. Pomeroy (2000), Advances in Canadian forest hydrology, 1995–1998, *Hydrol. Processes*, *14*(9), 1551–1578, doi:10.1002/1099-1085(20000630)14:9<1551::AID-HYP74>3.0.CO;2-J.

Buttle, J. M., I. F. Creed, and R. D. Moore (2005), Advances in Canadian forest hydrology, 1999–2003, *Hydrol. Processes*, *19*(1), 169–200, doi:10.1002/hyp.5773.

Caldwell, M. M., T. E. Dawson, and J. H. Richards (1998), Hydraulic lift: Consequences of water efflux from the roots of plants, *Oecologia*, *113*(2), 151–161, doi:10.1007/s004420050363.

Carey, S. K., and M. K. Woo (1999), Hydrology of two slopes in subarctic Yukon, Canada, *Hydrol. Processes*, *13*(16), 2549–2562, doi:10.1002/(SICI)1099-1085(199911)13:16<2549::AID-HYP938>3.0.CO;2-H.

Carey, S. K., and M. Woo (2001), Spatial variability of hillslope water balance, Wolf Creek Basin, subarctic Yukon, *Hydrol. Processes*, *15*(16), 3113–3132, doi:10.1002/hyp.319.

Cooper, P. J. M., J. D. H. Keatinge, and G. Hughes (1983), Crop evapotranspiration—A technique for calculation of its components by field measurements, *Field Crops Res.*, *7*(4), 299–312, doi:10.1016/0378-4290(83)90038-2.

dos Santos, G. H., and N. Mendes (2005), Unsteady combined heat and moisture transfer in unsaturated porous soils, *J. Porous Media*, *8*(5), 493–510, doi:10.1615/JPorMedia.v8.i5.70.

Engstrom, R., A. Hope, H. Kwon, D. Stow, and D. Zamolodchikov (2005), Spatial distribution of near surface soil moisture and its relationship to microtopography in the Alaskan arctic coastal plain, *Nord. Hydrol.*, *36*(3), 219–234.

Fosberg, M. A. (1975), Heat and water vapour flux in conifer forest litter and duff: A theoretical model, *Rep. RM-152*, 23 pp., For. Serv., U.S. Dep. of Agric., Washington, D. C.

Grayson, R. B., A. W. Western, F. H. S. Chiew, and G. Bloschl (1997), Preferred states in spatial soil moisture patterns: Local and nonlocal controls, *Water Resour. Res.*, *33*(12), 2897–2908, doi:10.1029/97WR02174.

Grifoll, J., J. M. Gasto, and Y. Cohen (2005), Non-isothermal soil water transport and evaporation, *Adv. Water Resour.*, *28*(11), 1254–1266, doi:10.1016/j.advwatres.2005.04.008.

Hillel, D. (1975), Simulation of evaporation from bare soil under steady and diurnally fluctuating evaporativity, *Soil Sci.*, *120*(3), 230–237, doi:10.1097/00010694-197509000-00011.

Hinzman, L. D., D. L. Kane, R. E. Gieck, and K. R. Everett (1991), Hydrological and thermal properties of the active layer in the Alaskan arctic, *Cold Reg. Sci. Technol.*, *19*(2), 95–110, doi:10.1016/0165-232X(91)90001-W.

Jackson, R. D., B. A. Kimball, R. J. Reginato, and F. S. Nakayama (1973), Diurnal soil-water evaporation - time-depth-flux patterns, *Soil Sci. Soc. Am. J.*, *37*(4), 505–509.

Jackson, R. D., R. J. Reginato, B. A. Kimball, and F. S. Nakayama (1974), Diurnal soil-water evaporation—Comparison of measured and calculated soil-water fluxes, *Soil Sci. Soc. Am. J.*, *38*(6), 861–866.

Jackson, R. D., S. B. Idso, and R. J. Reginato (1976), Calculation of evaporation rates during transition from energy-limiting to soil-limiting phases using albedo data, *Water Resour. Res.*, *12*(1), 23–26, doi:10.1029/WR012i001p00023.

Jacobs, A. F. G., B. G. Heusinkveld, R. J. W. Kruit, and S. M. Berkowicz (2006), Contribution of dew to the water budget of a grassland area in the Netherlands, *Water Resour. Res.*, *42*, W03415, doi:10.1029/2005WR004055.

Johnson, E. A. (1992), *Fire and Vegetation Dynamics: Studies From the North American Boreal Forest*, 129 pp., doi:10.1017/CBO9780511623516, Cambridge Univ. Press, Cambridge, U. K.

Keith, D. M. (2008), Temporal and spatial processes controlling the duff water budget: Experimental and model evidence, MS thesis, 189 pp., Dep. of Biol. Sci., Univ. of Calgary, Calgary, Alberta, Canada.

Kim, H. J., R. C. Sidle, and R. D. Moore (2005), Shallow lateral flow from a forested hillslope: Influence of antecedent wetness, *Catena*, *60*(3), 293–306, doi:10.1016/j.catena.2004.12.005.

Laurén, A., and H. Mannerkoski (2001), Hydraulic properties of mor layers in Finland, *Scand. J. For. Res.*, *16*(5), 429–441, doi:10.1080/02827580152632829.

Laurén, A., H. Mannerkoski, and T. Orjasniemi (2000), Thermal and aeration properties of mor layers in Finland, *Scand. J. For. Res.*, *15*(4), 433–444, doi:10.1080/028275800750172655.

Liu, B. C., W. Liu, and S. W. Peng (2005), Study of heat and moisture transfer in soil with a dry surface layer, *Int. J. Heat Mass Transfer*, *48*(21–22), 4579–4589.

Luikov, A. V. (1975), Systems of differential equations of heat and mass-transfer in capillary-porous bodies, *Int. J. Heat Mass Transfer*, *18*(1), 1–14, doi:10.1016/0017-9310(75)90002-2.

Maraun, D., and J. Kurths (2004), Cross wavelet analysis: Significance testing and pitfalls, *Nonlinear Processes Geophys.*, *11*(4), 505–514, doi:10.5194/npg-11-505-2004.

McDonnell, J. J., I. F. Owens, and M. K. Stewart (1991), A case-study of shallow flow paths in a steep zero-order basin, *Water Resour. Bull.*, *27*(4), 679–685.

Millington, R., and J. P. Quirk (1961), Permeability of porous solids, *Trans. Faraday Soc.*, *57*(8), 1200–1207, doi:10.1039/tf9615701200.

Milly, P. C. D. (1984), A simulation analysis of thermal effects on evaporation from soil, *Water Resour. Res.*, *20*(8), 1087–1098, doi:10.1029/WR020i008p01087.

Miyanishi, K. (2001), Duff consumption, in *Forest Fires: Behavioural and Ecological Effects*, edited by E. A. Johnson and K. Miyanishi, pp. 437–475, Academic, San Diego, Calif.

Miyanishi, K., and E. A. Johnson (2002), Process and patterns of duff consumption in the mixedwood boreal forest, *Can. J. For. Res.*, *32*(7), 1285–1295, doi:10.1139/x02-051.

Narasimhan, T. N., and P. A. Witherspoon (1976), Integrated finite difference method for analyzing fluid flow in porous media, *Water Resour. Res.*, *12*(1), 57–64, doi:10.1029/WR012i001p00057.

Nash, J. E., and J. V. Sutcliffe (1970), River flow forecasting through conceptual models part i—A discussion of principles, *J. Hydrol.*, *10*(3), 282–290, doi:10.1016/0022-1694(70)90255-6.

Penman, H. L. (1948), Natural evaporation from open water, bare soil and grass, *Proc. R. Soc. A*, *193*(1032), 120–145, doi:10.1098/rspa.1948.0037.

Perry, R. H., D. W. Green, and J. O. Maloney (Eds.) (1984), *Perry's Chemical Engineers' Handbook*, 6th ed., McGraw Hill, Toronto.

Philip, J. R., and D. A. De Vries (1957), Moisture movement in porous materials under temperature gradients, *Eos Trans. AGU*, *38*(2), 222.

Pruess, K. (1999), Tough2 user's guide, version 2.0, *Rep. LBNL-43134*, 197 pp., Lawrence Berkeley Lab., Berkeley, Calif.

Pruess, K. (2004), The tough codes—A family of simulation tools for multiphase flow and transport processes in permeable media, *Vadose Zone J.*, *3*(3), 738–746, doi:10.2113/3.3.738.

Raaflaub, L. D., and C. Valeo (2008), Assessing factors that influence spatial variations in duff moisture, *Hydrol. Processes*, *22*(15), 2874–2883, doi:10.1002/hyp.7075.

Ritchie, J. T. (1981), Water dynamics in the soil-plant-atmosphere system, *Plant Soil*, *58*(1–3), 81–96, doi:10.1007/BF02180050.

Samran, S., P. M. Woodard, and R. L. Rothwell (1995), The effect of soil-water on ground fuel availability, *For. Sci.*, *41*(2), 255–267.

Sidle, R. C., S. Noguchi, Y. Tsuboyama, and K. Laursen (2001), A conceptual model of preferential flow systems in forested hillslopes: Evidence of self-organization, *Hydrol. Processes*, *15*(10), 1675–1692, doi:10.1002/hyp.233.

Soil Classification Working Group (1998), *The Canadian System of Soil Classification*, *Agric. Agric. Food Can. Publ.*, vol. 1646, 187 pp., NRC Res. Press, Ottawa.

Stevenson, D. R. (1967), *Geological and Groundwater Investigations in the Marmot Creek Experimental Basin of Southwestern Alberta, Canada*, 106 pp., Univ. of Alberta, Edmonton, Alberta, Canada.

Strahler, A. N. (1957), Quantitative analysis of watershed geomorphology, *Eos Trans. AGU*, *8*(6), 913.

Tamai, K., T. Abe, M. Araki, and H. Ito (1998), Radiation budget, soil heat flux and latent heat flux at the forest floor in warm, temperate mixed forest, *Hydrol. Processes*, *12*(13–14), 2105–2114, doi:10.1002/(SICI)1099-1085(19981030)12:13/14<2105::AID-HYP723>3.0.CO;2-9.

Torrence, C., and G. P. Compo (1998), A practical guide to wavelet analysis, *Bull. Am. Meteorol. Soc.*, *79*(1), 61–78, doi:10.1175/1520-0477(1998)079<0061:APGTWA>2.0.CO;2.

Van Cleve, K., L. Oliver, R. Schlentner, L. A. Viereck, and C. T. Dyrness (1983), Productivity and nutrient cycling in taiga forest ecosystems, *Can. J. For. Res.*, *13*(5), 747–766, doi:10.1139/x83-105.

Van Wagner, C. E. (1979), A laboratory study of weather effects on the drying rate of jack pine litter, *Can. J. For. Res.*, *9*, 267–275, doi:10.1139/x79-044.

Van Wagner, C. E. (1982), Initial moisture content and the exponential drying process, *Can. J. For. Res.*, *12*, 90–92, doi:10.1139/x82-013.

Vo, S. (2001), Duff water balance in the Canadian boreal forest, M.Sc. thesis, 106 pp, Univ. of Calgary, Calgary, Alberta, Canada.

Weiss, R., J. Alm, R. Laiho, and J. Laine (1998), Modeling moisture retention in peat soils, *Soil Sci. Soc. Am. J.*, *62*(2), 305–313.

Western, A. W., G. Bloschl, and R. B. Grayson (1998), Geostatistical characterization of soil moisture patterns in the Tarrawarra catchment, *J. Hydrol.*, *205*(1–2), 20–37, doi:10.1016/S0022-1694(97)00142-X.

Western, A. W., R. B. Grayson, G. Bloschl, G. R. Willgoose, and T. A. McMahon (1999), Observed spatial organization of soil moisture and its relation to terrain indices, *Water Resour. Res.*, *35*(3), 797–810, doi:10.1029/1998WR900065.

Yamanaka, T., and T. Yonetani (1999), Dynamics of the evaporation zone in dry sandy soils, *J. Hydrol.*, *217*(1–2), 135–148, doi:10.1016/S0022-1694(99)00021-9.

E. A. Johnson and D. M. Keith, Department of Biological Sciences, University of Calgary, Calgary, Alberta T2N 1N4, Canada.

C. Valeo, Department of Civil Engineering, Schulich School of Engineering, University of Calgary, Calgary, Alberta T2N 1N4, Canada. (valeo@ucalgary.ca)